Koulin G, Reavie T, Frazer R, Shaw BA.

Economic method for helical gear flank surface characterisation.

***Surface Topography: Metrology and Properties* 2017,**

https://doi.org/10.1088/2051-672X/aaa0f2

Economic method for helical gear flank surface characterisation

G Koulin, T Reavie, RC Frazer and BA Shaw
Design Unit, School of Engineering, Newcastle University, Newcastle upon Tyne, NE1 7RU, United Kingdom

E-Mail: giorge.koulin@ncl.ac.uk

Abstract. Typically the quality of a gear pair is assessed based on simplified geometric tolerances which do not always correlate with functional performance. In order to identify and quantify functional performance based parameters, further development of the gear measurement approach is required. Methodology for interpolation of the full active helical gear flank surface, from sparse line measurements, is presented. The method seeks to identify the minimum number of line measurements required to sufficiently characterise an active gear flank. In the form ground gear example presented, a single helix and three profile line measurements was considered to be acceptable. The resulting surfaces can be used to simulate the meshing engagement of a gear pair and therefore provide insight into functional performance based parameters. Therefore the assessment of the quality can be based on the predicted performance in the context of an application.

PACS: 06.20.-f; 02.60.Ed

Keywords: helical gear surface, gear measurement, gear functionality, geometric product specification

1 Introduction

Current gear measurement practice employs the simple pass or fail approach, where the gears are accepted or rejected based on tolerance limit values specified in standards [1]. The evaluation parameters used to quantify the quality of the gear are applied to a single involute profile line scan and a single helix line scan in the middle of the face width and roll length, respectively.

The whole gear flank surface is involved in the gear mesh engagement action, therefore a single lead and helix is potentially an over-simplification of the active tooth surface. Additionally, the contact lines during tooth engagement cross the active gear flank diagonally on helical gears, resulting in point intersections with profile and helix measurements. Therefore this traditional measurement approach may not always correlate well with performance of a gear pair, even though standard practice in gear design is to use these simplified measurements to estimate dynamic factor K_V and face load factor $K_{H\beta}$ affecting performance [2]. Dynamic factor K_V is an estimate of the self induced increase of total mesh torque at operating speed of manufactured gears when compared with the mesh torque of ideal gears

having zero transmission error. Face load factor $K_{H\beta}$ is an estimate of maximum load intensity per unit face width when compared with the average load per unit face width caused by mesh misalignment.

Traditional profile and helix line scanning does provide useful information to set and adjust manufacturing machine tools. Some manufacturing processes such as form grinding or power honing can introduce a variability of profile and helix manufacturing errors known as twist or torsion. Gear measuring machine manufactures provide options where three profiles and three helices are measured on a single tooth. This method is able to quantify known manufacturing error trends but is not focussed on gear performance characterisation.

A series of international organisation for standardisation (ISO) standards have been developed to address geometric product specification (GPS) [3]. GPS requires that the functional performance based geometrical parameters are specified and quantified. In terms of gears, the functionality includes contact and bending stresses, scuffing resistance, efficiency, noise and vibration which are excited by kinematic error known as transmission error (TE). There is some correlation of gear mesh functionality and performance with the simplified single profile and helix measurements however this does not capture the full complexity. One possible way to both identify and quantify these functional geometrical parameters is through tooth contact analysis (TCA) [4]. TCA simulates the rolling contact of the gear mesh under load and can predict stresses, efficiency and TE. TCA models vary in complexity and performance and require verification with extensive testing for each gear application.

In order to satisfy GPS, the quantification of the quality of a gear pair would ideally involve: measuring the full contacting surfaces of the gear pair and simulating the contact by means of TCA. Further development in full contact surface characterisation is necessary in order to fulfil this criteria. Attempts at gear flank surface characterisation in 3D have already been made [5, 6]. Unfortunately these methods have not been adopted as standard practice for practical applications to date.

This article presents a methodology that can be used to characterise the whole contact surface of a helical gear and to generate the surface data necessary for import to a validated TCA. The method is demonstrated on the profile and helix measurement results acquired by a dedicated gear measurement machine (GMM), which is a contacting stylus instrument that is standard practice in the industry [7]. The method essentially interpolates profile and helix measurements to simulate the whole gear flank surface. The method estimates the minimum measurements necessary in order to sufficiently but economically characterise the whole gear flank surface. Gear measurement is time consuming and costly so minimising measurement time is very important for gear manufacturers.

2 Methodology

A method has been developed which allows the characterisation of the whole active helical gear flank surface from a number of sparse line measurements. The aim of the method is such that the surface can be characterised sufficiently yet economically using minimum number of single line measurements. The surface resulting from the application of this method is useful for modelling gear pair performance by means of TCA or similar techniques.

2.1 Measurement system

The method has been developed to utilise GMM measurement results, which is the current practice in power transmission industry. However the principles presented here can be expanded to be used with other types of measurements. A Klingelnberg P65 GMM was used to obtain the gear measurements. This is a standard 4-axis GMM which uses involute generation measurement method to measure gear profile form deviations. This particular machine is the UK's primary gear measuring machine in the National Gear Metrology Laboratory and has traceability to Physikalisch-Technische Bundesanstalt, Germany for involute gear measurement. Measurement uncertainties $U(k=2)$ are ± 1.2 µm for total profile deviation F_α and profile form deviation $f_{f\alpha}$; ± 1.0 µm for profile slope deviation $f_{H\alpha}$; ± 1.3 µm for total helix deviation F_β and helix form deviation $f_{f\beta}$; and ± 1.0 µm for helix slope deviation $f_{H\beta}$. Each profile and helix measurement was comprised of 480 measurement points. A stylus with a 2.0 mm diameter ball ruby tip was used and a Gaussian filter applied in accordance with the standard [1].

2.2 Example helical gear

The methodology was tested on an example precision ground helical gear. For the purpose of examining and validating of the method, a single flank of the example gear was measured. The main geometry parameters of the example helical gear are summarised in Table 1. This particular gear serves as a good example since it has both profile and helix modifications and also a twist error from the manufacturing process.

Table 1: Nominal involute helical gear geometry parameters.

Parameter	Value
Number of teeth	23
Face width	44 mm
Normal module	6 mm
Reference pressure angle	20°
Reference helix angle	28.1°
Hand of helix	left
Tip diameter or end of active profile (EAP)	168.764 mm
Reference diameter	156.440 mm
Root diameter	139.697 mm
Start of active profile (SAP) diameter	148.481 mm
Start of tip relief (STR) diameter	162.072 mm
Tip relief	Linear 50 µm
Helix crowning	Parabolic 15 µm

The example gear was measured on the GMM. Forty profile measurements equally spaced along the face width and a single helix measurement at the reference diameter were acquired. This type of measurement is referred to as topography measurement in the context of this paper. The topography measurement is used as the representation of the full helical gear flank surface and serves as the bench mark reference against which the subsequent interpolated surfaces are compared. A point to point difference between topography and interpolated surfaces is calculated. The standard deviation of the

difference is used to quantify the quality of the interpolated surface and thus the measurement and interpolation strategy.

2.3 Interpolation model

Precision grinding of gears results in an anisotropic surface, which has strong directionality. The grinding marks or lays left by the motion of the grinding wheel typically span the whole flank from one side to the other along the helix direction. The method interpolates between profile measurements therefore exploiting the directionality of the surface.

The interpolation of the flank surface is achieved with the use of weighting functions. Each measured profile has a single weighting function associated with it. An interpolated profile is the sum of the products of measured profiles and their weighting functions at the interpolated profile's face width position. The weighting functions were constructed to satisfy the following rules:

1. At the face width where the measured profile is located the function weighting must be 100 %.
2. At the face width half way between the next or previous measured profile the function weighting must be 50 %.
3. At the face width where the next or previous profile is located the function weighting must be 0 % or ~ 0 %.
4. At any given point along the face width the sum of all of the weighting functions must be 100 %.

It is also assumed that the profiles need not to be equally spaced. The application of this method allows the use of additional profile measurements near the locations of steeper change, for example at the edges of face width where chamfers may be present or areas of pitting for worn profiles, etc.

Any weighting function can be used provided it satisfies the weighting function construction rules. Two weighting functions were used to test the process but other weighting functions may prove more effective. As a first example a simple linear interpolation function was used. The linear weighting functions for an arbitrary profile and its immediate neighbours are illustrated in Figure 1. Where *w(b)* is a weighting function of face width position *b* and subscript *i* is the identifier corresposnding to a measured profile and takes whole numbers only.

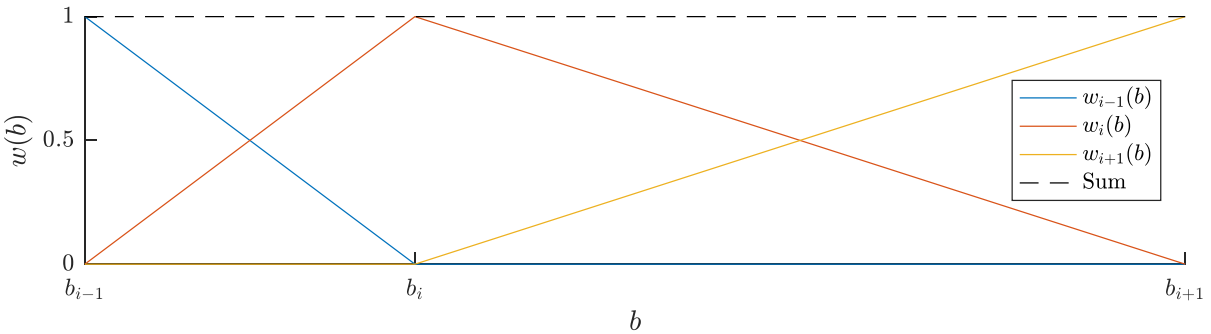

Figure 1: Linear interpolation weighting functions.

Gaussian function forms the basis of the second weighting function. This was selected to place more emphasis on the nearest measured profiles and thus may more accurately capture local features for form grinding.

$$g(b) = \exp\left(-\frac{(b-\mu)^2}{2\sigma^2}\right) \tag{1}$$

where *g(b)* is the Gaussian as a function of face width *b*, μ is the mean value about which the Gaussian function is centred and σ^2 is the variance, which can be calculated if *g(b)* is known at a specific *b*:

$$\sigma = \frac{b-\mu}{\sqrt{-2ln\big(g(b)\big)}} \tag{2}$$

For a measured profile located at b_i the Gaussian becomes:

$$g_i(b) = \exp\left(-\frac{(b-b_i)^2}{2{\sigma_i}^2}\right) \tag{3}$$

To satisfy construction rule 3 variance is calculated from equation (2) for the case of $g_i(b_{i+1}) = 0.001$ which is equivalent to $\mu + 3.29\sigma$ interval. To accommodate for unequal spacing between selected profiles a difference is made between upper and lower parts of the Gaussian which must have differing variance in order to satisfy the weighting response mentioned above:

$$\sigma_i = \begin{cases} \dfrac{b_{i+1}-b_i}{\sqrt{-2ln(0.001)}} & for\ \ \{b \in \mathbb{R} \mid b \geq b_i\} \\ \dfrac{b_i-b_{i-1}}{\sqrt{-2ln(0.001)}} & for\ \ \{b \in \mathbb{R} \mid b < b_i\} \end{cases} \tag{4}$$

where b_{i+1} and b_{i-1} are upper and lower neighbours with respect to the measured profile located at b_i, respectively. The resulting Gaussian functions are illustrated in Figure 2(a). These functions satisfy construction rules 1 and 3, however they do not satisfy rules 2 and 4. We have to modify the Gaussian functions in order to achieve the required response.

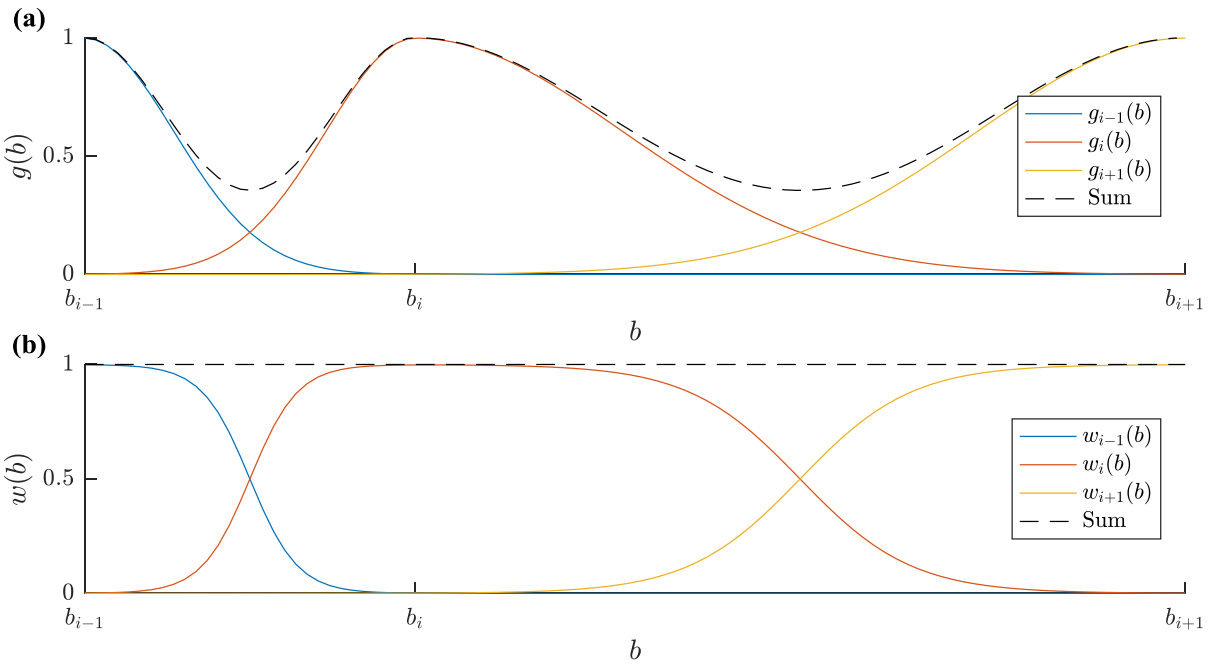

Figure 2: Gaussian interpolation weighting functions. (a) Uneven Gaussian distributions. (b) Modified Gaussian weighting functions.

In order to produce the required response each Gaussian function is normalised by the total sum of the functions:

$$w_i(b) = \frac{g_i(b)}{\sum_{j=1}^{n} g_j(b)} \tag{5}$$

where $w_i(b)$ is the modified Gaussian weighting function corresponding to the measured profile located at b_i, n is the total number of measured profiles and subscript j is substituted in place of subscript i in order to allow the summing operation. The resulting weighting functions are shown in Figure 2(b), which satisfy all of the construction rules. This weighting function is similar to cumulative distribution function. Rule 3 implies that the major contribution to the sum of the Gaussian functions partway between two measured profiles comes from the two neighbouring functions. Therefore equation (5) can be further simplified:

$$w_i(b) \cong \frac{g_i(b)}{g_{i+1}(b) + g_i(b) + g_{i-1}(b)} \quad for \ \{b \in \mathbb{R} \mid b_{i+1} \geq b \geq b_{i-1}\} \tag{6}$$

Now consider interpolating for a profile located partway between two measured profiles, illustrated in Figure 3. This is done by summing the products of the selected profiles and their weighting functions:

$$P_{i+a} = \sum_{j=1}^{n} P_j w_j(b_{i+a}) \quad for \ \{a \in \mathbb{R} \mid 1 > a > 0\} \tag{7}$$

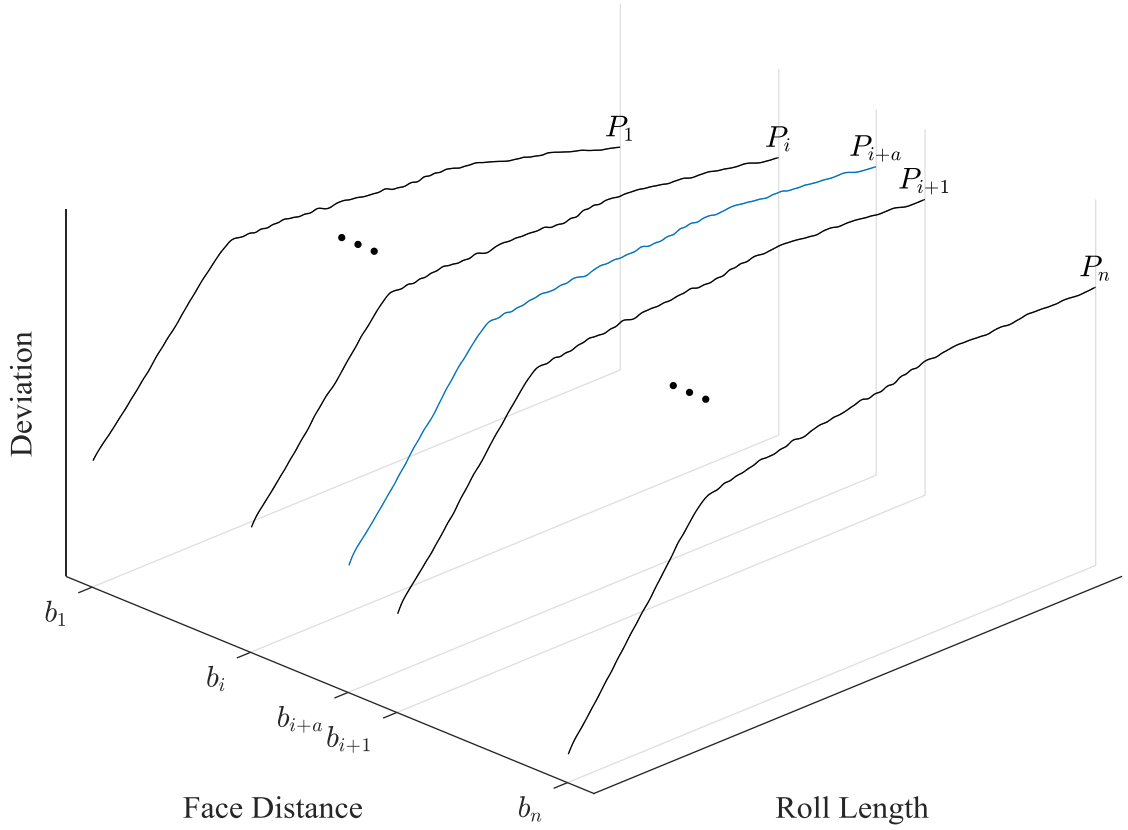

Figure 3: Measured and interpolated profiles labelled *P*. Measured profiles are indicated by whole number subscripts, where *n* is the total number of measured profiles and subscript *i* can only take whole numbers. Interpolated profiles are placed between measured profiles and are indicated real number subscripts, where subscript *a* is a real number in the range $1 > a > 0$.

where P_j is a measured profile located at face width b_j and P_{i+a} is an interpolated profile located at face width b_{i+a}. Applying construction rule 3, the equation can be simplified to include only two weighted profile products since the contribution from other weighted profiles is negligible.

$$P_{i+a} \cong P_i w_i(b_{i+a}) + P_{i+1} w_{i+1}(b_{i+a}) \quad for \ \{a \in \mathbb{R} \mid 1 > a > 0\} \tag{8}$$

2.4 Interpolation with form removal

Up to now the described method interpolates both the form and waviness together. Where the form describes micro corrections such as crowning and tip relief, and contains manufacturing errors. The waviness describes the undulations of the surface texture of the higher frequency than the form. This general description of the form and waviness has some exceptions, for example the discontinuity created by the start of linear tip relief which is in the higher frequency domain of the waviness.

It is possible to separate the waviness from the form, interpolate the waviness component and then reapply the extracted form. This can improve the quality of the resulting interpolation surface. A surface polynomial has been used to define the form, a process which is routinely used in metrology. The residuals remaining after form removal are defined as waviness in this context. Some selected surface polynomial equations are summarised in Table 2.

Table 2: Polynomial surface equations

Polynomial order		Polynomial surface equation
Face width	Roll length	
1	1	$S_{11}(b,\rho) = c_{10}b + c_{01}\rho + c_{00}$
2	2	$S_{22}(b,\rho) = c_{20}b^2 + c_{02}\rho^2 + c_{11}b\rho + S_{11}$
3	3	$S_{33}(b,\rho) = c_{30}b^3 + c_{03}\rho^3 + c_{21}b^2\rho + c_{12}b\rho^2 + S_{22}$
5	5	$S_{55}(b,\rho) = c_{50}b^5 + c_{05}\rho^5 + c_{41}b^4\rho + c_{14}b\rho^4 + c_{32}b^3\rho^2 + c_{23}b^2\rho^3 + c_{40}b^4 + c_{04}\rho^4 + c_{31}b^3\rho + c_{13}b\rho^3 + c_{22}b^2\rho^2 + S_{33}$

where S_{ij} is the polynomial surface equation, b is the facewidth, ρ is the roll length, c_{ij} is a numerical constant which defines a specific fitting function, subscripts i and j are order of polynomial in facewidth and roll length, respectively.

2.5 Method uncertainty

While the uncertainty of individual profile and helix line measurements are known, the uncertainty of the surface characterisation process is yet to be evaluated.

3 Results & discussions

The topography measurement results of the example helical gear is illustrated in Figure 4. The measured topography data is used as the reference for evaluating the surface generation process. In addition to tip relief and helix crowning modifications, the flank exhibits a linear twist manufacturing error. At least one helix measurement is necessary to align profile measurements relative to each other. In order to simulate a measurement set at a lower sampling in the face width, five profiles were arbitrarily selected from the topography data set in order to test the methodology. Depending on manufacturing process, gear design and quality, the minimum profiles needed to characterise the gear flank surface requires investigation for each case. The authors have investigated an example of a form ground manufactured gear and the results are discussed in the following sections.

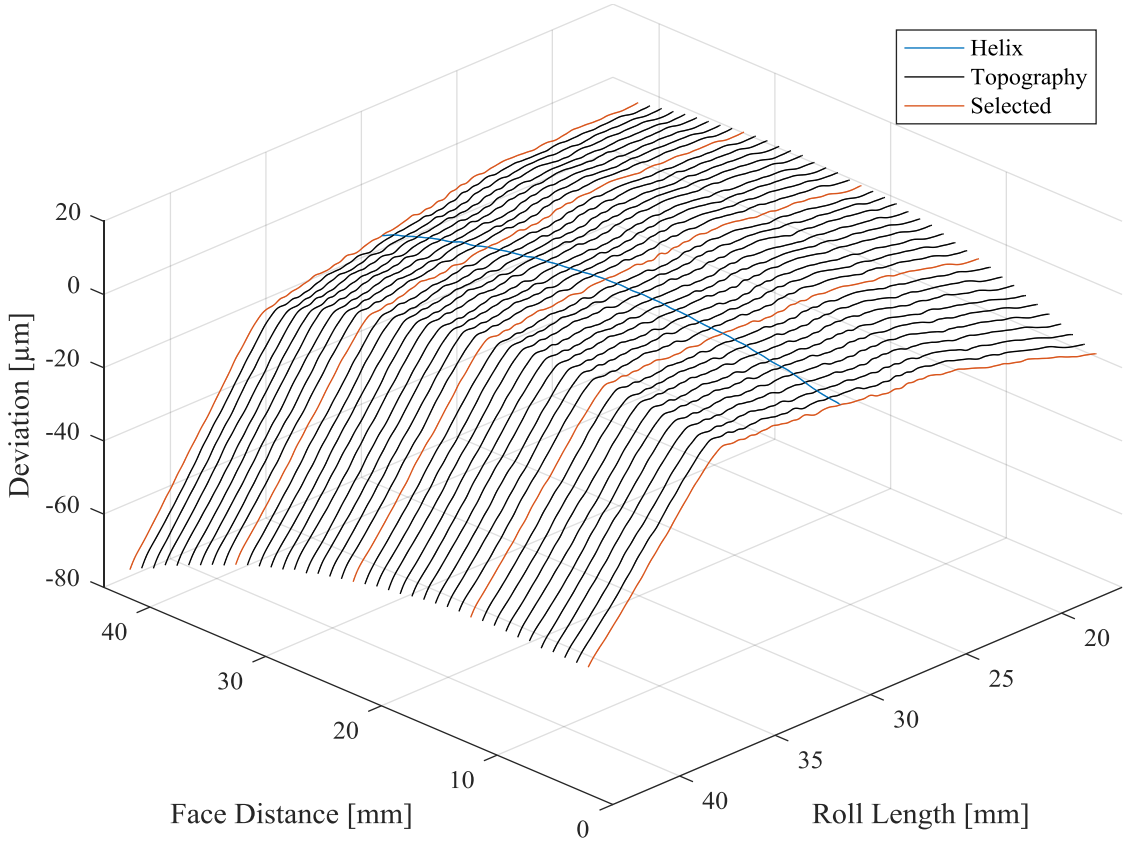

Figure 4: Gear flank topography measurement results including 40 profiles and a single helix lines. The single helix measurement is used to align the profiles relative to each other. A number of profiles are selected to simulate a measurement with fewer profiles.

3.1 Interpolation

Firstly the linear interpolation is applied to the reduced data set of five profiles and a single helix line measurements. The resulting interpolated and topography surfaces are illustrated in Figure 5. The topography surface is defined by the discrete measurement points as illustrated in Figure 4. For the visual representation of the surface the fragments between those discrete points are interpolated graphically but are not used in further evaluation. The interpolated surface is defined in similar manner, employing the same roll length and face width grid spacing as the topography surface to enable point to point comparison. The deviations of the interpolated surface have been exaggerated for illustration purposes, an arbitrarily chosen factor of ten scaling seemed to provide suitable visualisation. This scaling factor has been applied with respect to the topography surface.

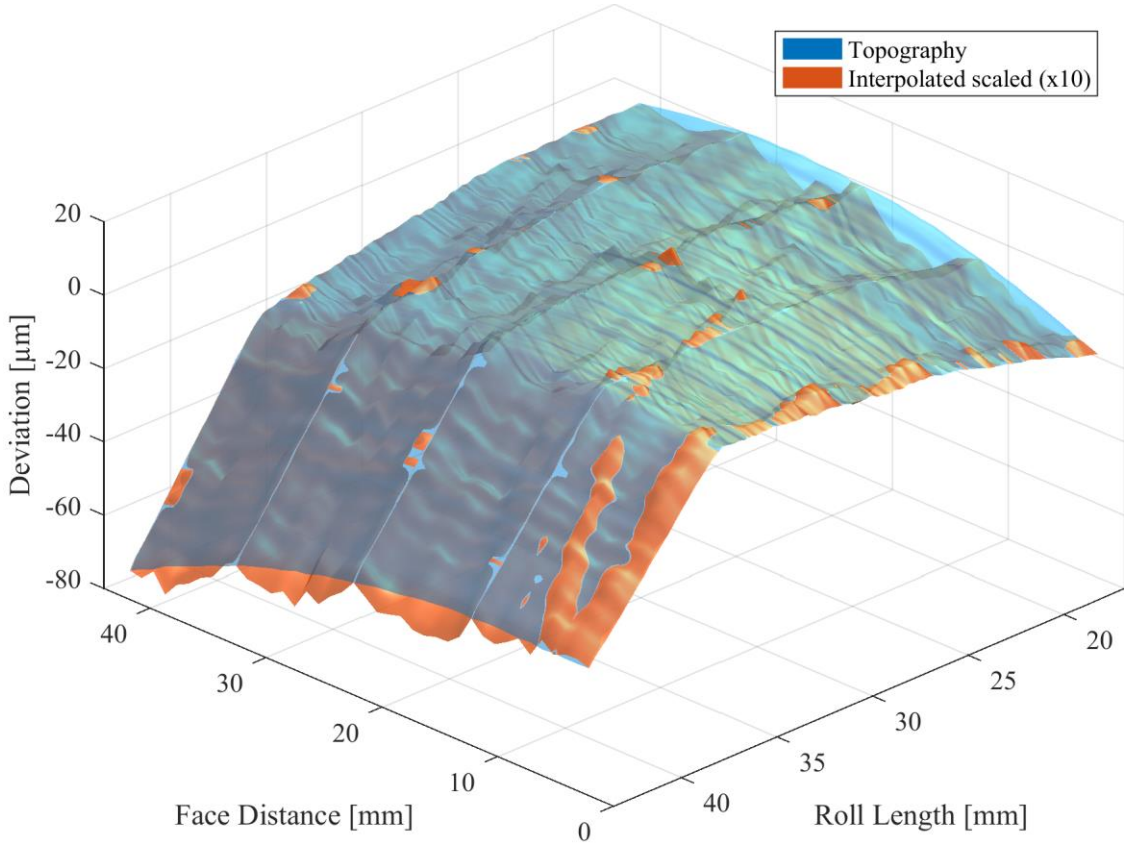

Figure 5: Measured topography and linear interpolated flank surfaces. The deviations of the interpolated surface have been scaled by factor of 10 with respect to the topography surface.

The quality of the linear interpolated surface is assessed by evaluating the difference with the topography surface which serves as a reference, see Figure 6. This difference is a measure of how well the interpolated surface represents the measured topography and therefore the real surface. The quality of the interpolated surface is quantified by the standard deviation of this evaluated difference. The standard deviation of the difference can be used to estimate the uncertainty. The uncertainty resulting from the application of the interpolation method which provides additional contribution to the overall measurement uncertainty. The larger the differences between the interpolated points and the measured reference topography points, the greater the contribution from the interpolation method to the overall measurement uncertainty. Notice that the five lines of zero difference correspond to the five profiles which were selected from the topography dataset and therefore correspond exactly.

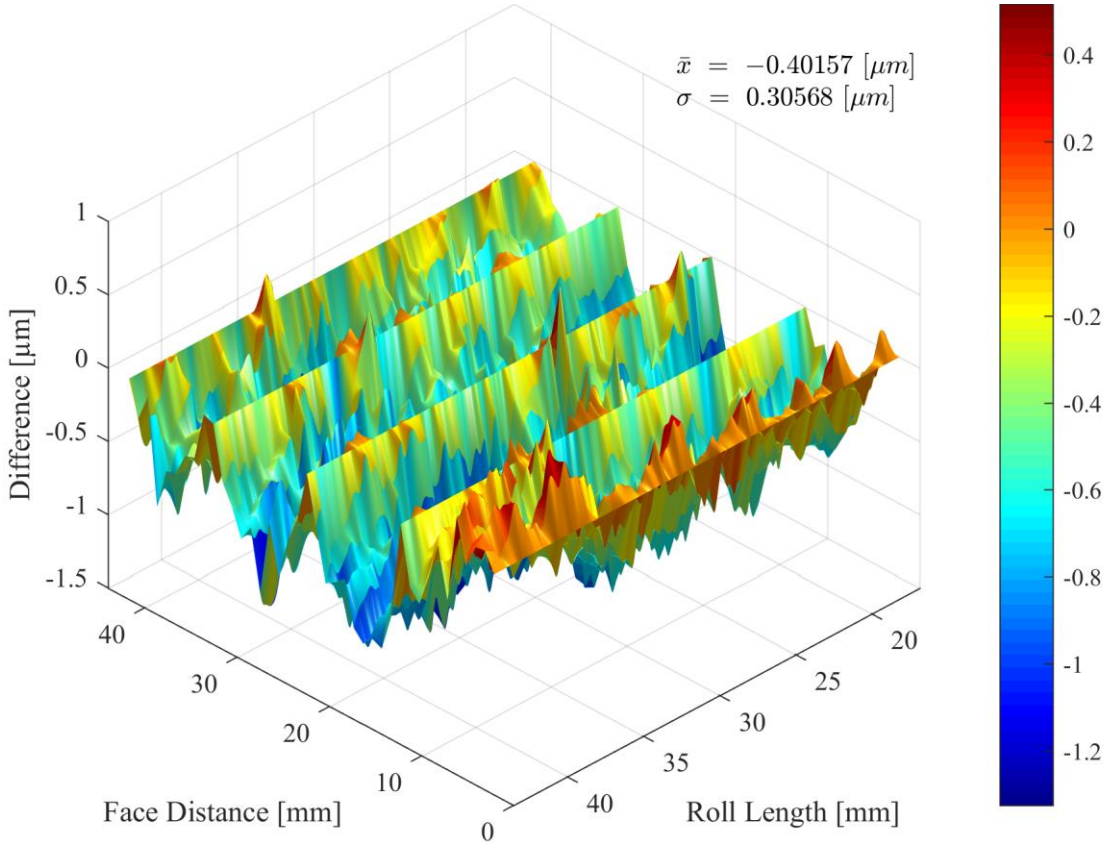

Figure 6: Difference between the topography and linear interpolated surfaces. Standard deviation of the difference σ = 0.31 µm.

Applying the Gaussian interpolation to the reduced data set, yields the interpolated surface illustrated in Figure 7. The deviations of the interpolated surface have been exaggerated for illustration purposes, a factor of ten scaling has been applied with respect to the topography surface. The Gaussian interpolation provides a greater weighting towards the measured data resulting in the ripples of the interpolated surface. The quality of the Gaussian interpolated surface is assessed by evaluating the difference with the topography surface, illustrated in Figure 8.

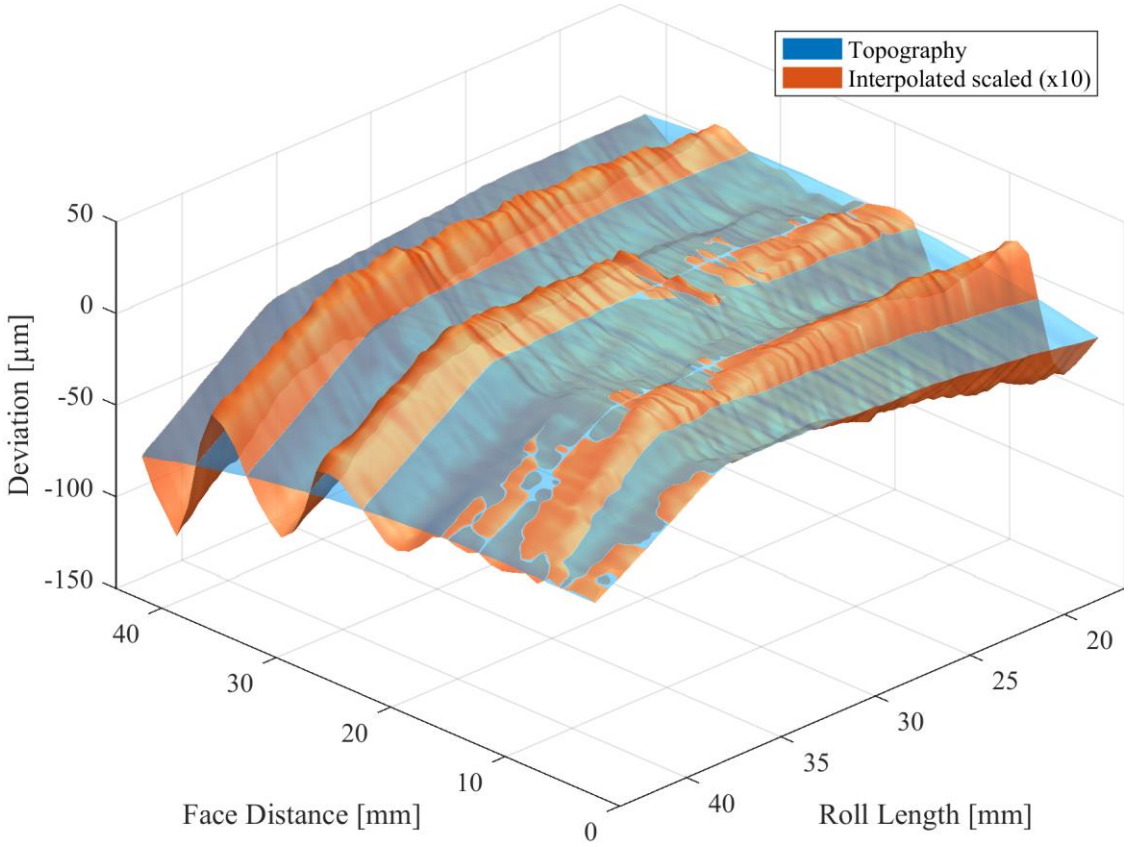

Figure 7: Topography and Gaussian interpolated flank surfaces. The deviations of the interpolated surface have been scaled by factor of 10 with respect to the topography surface.

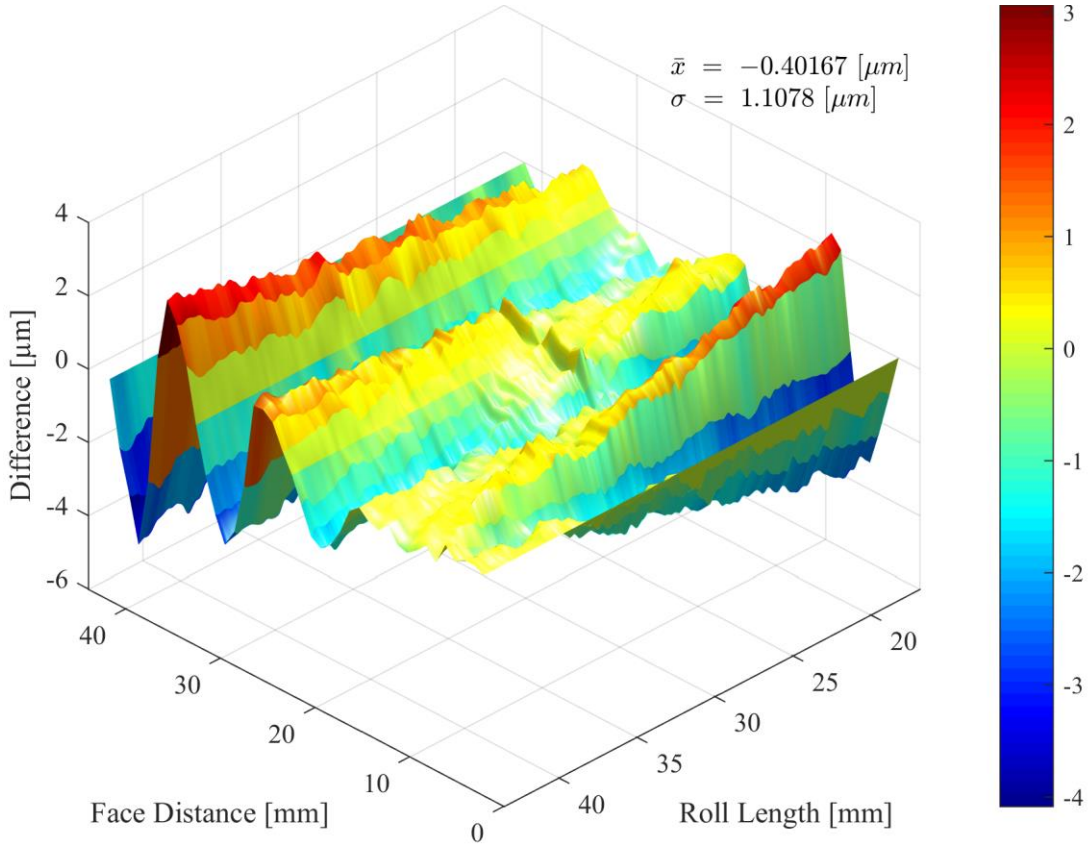

Figure 8: Difference between the topography and Gaussian interpolated surfaces. Standard deviation of the difference σ = 1.11 µm.

The resulting standard deviation of the differences is 0.31 µm and 1.11 µm for linear and Gaussian interpolation, respectively as stated in Figure 6 and Figure 8. Large discrepancy between these two values results from the underlying form of the flank. Linear interpolation produces a smoother interpolation of the underlying form. On the other hand Gaussian interpolation weights more heavily towards the measured data and its form therefore the resulting interpolation is less smooth exhibiting ripples over the difference surface.

3.2 Interpolation with form removal

So far we have interpolated both the form and waviness together. It is possible to separate the waviness from the form, interpolate the waviness and then reapply the extracted form. A linear least squares approach was used to fit $S_{55}(b, \rho)$ surface polynomial to the reduced data set. The resulting form surface is illustrated in Figure 9. Extracting the form from the measurement leaves the residual waviness of the surface. This residual waviness is linearly interpolated, the results are illustrated in Figure 10. Reapplying the extracted form to the interpolated waviness produced the interpolation surface illustrated in Figure 11. The quality of the interpolated surface is assessed by evaluating the difference with the topography surface, illustrated in Figure 12.

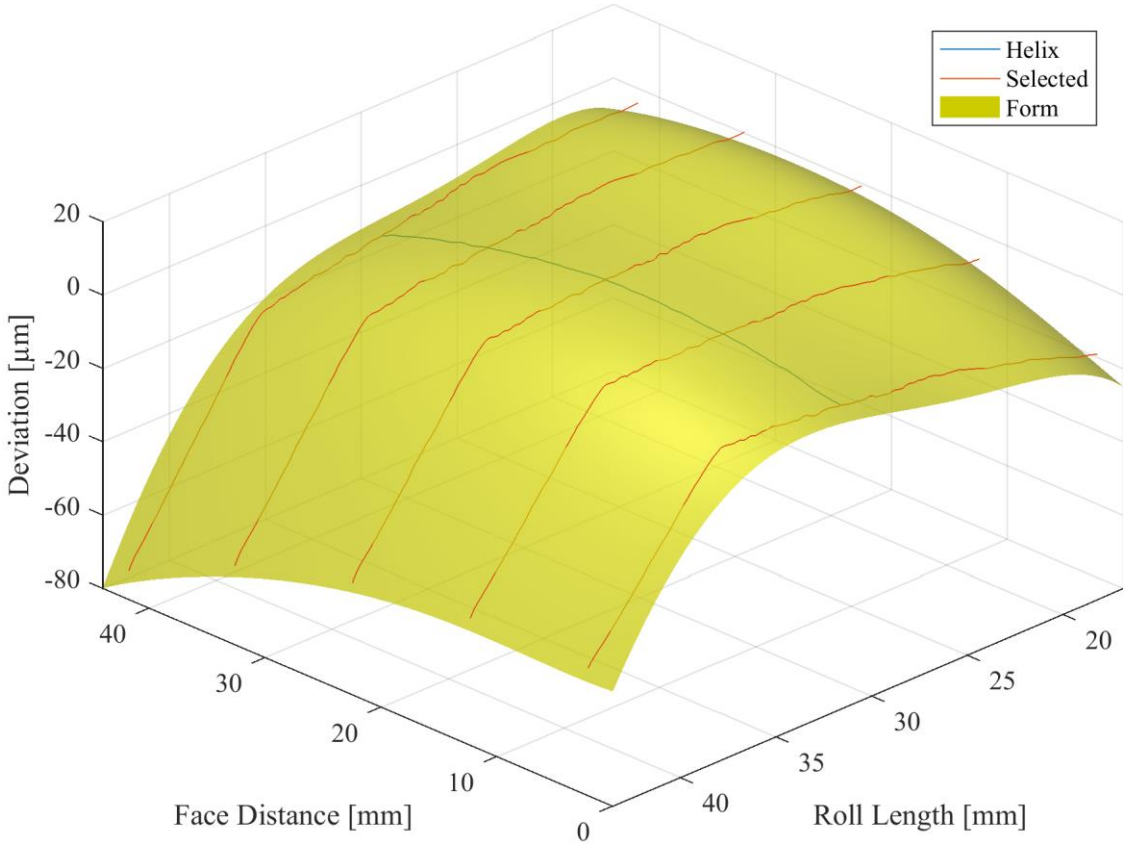

Figure 9: $S_{55}(b, \rho)$ surface polynomial fit of the form.

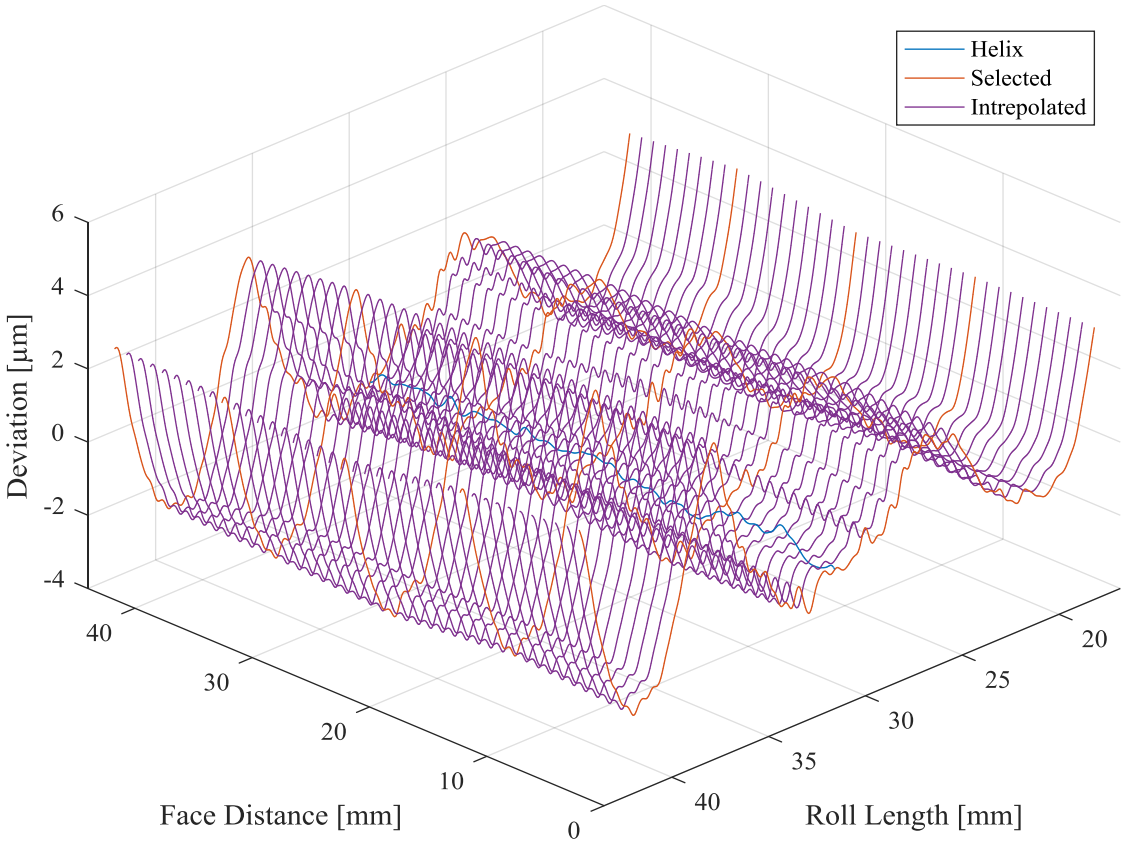

Figure 10: Waviness residual after removing $S_{55}(b, \rho)$ description of the form. Linear interpolation of the waviness is also shown.

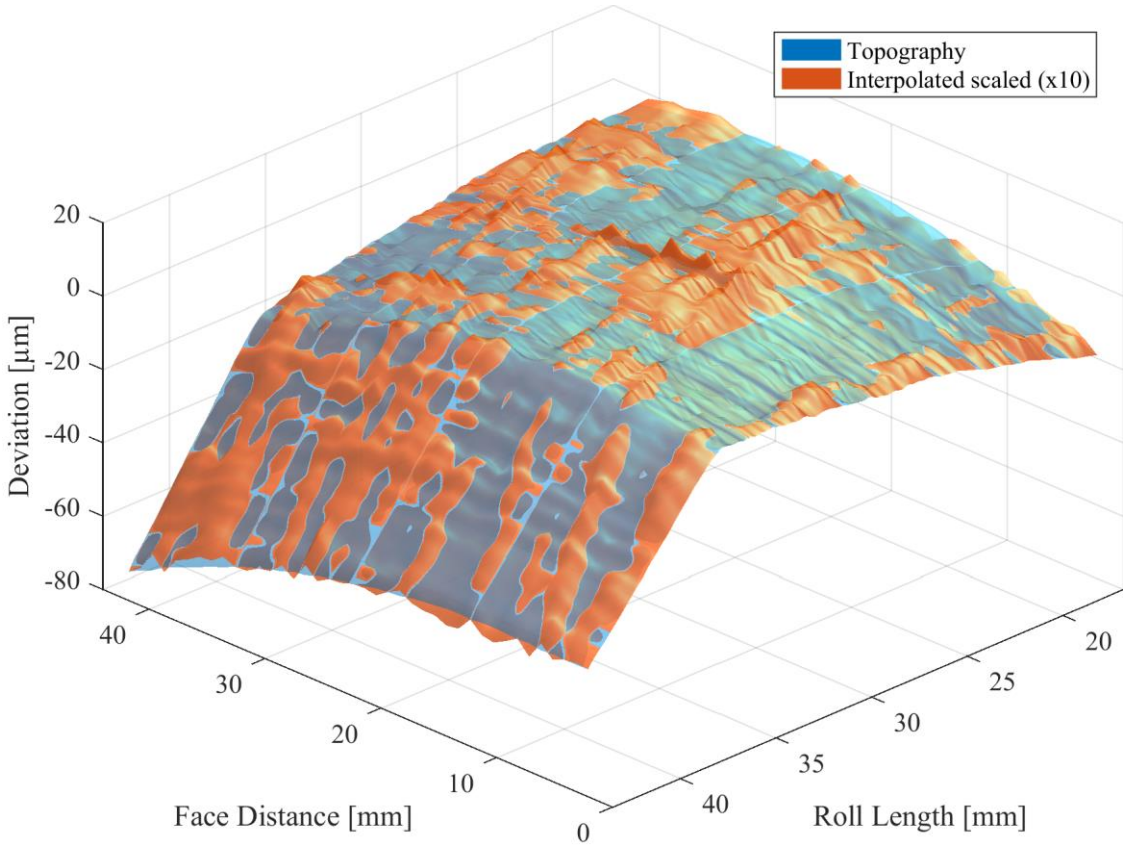

Figure 11: Topography and linear interpolated flank surfaces with form removal. The deviations of the interpolated surface have been scaled by factor of 10 with respect to the topography surface.

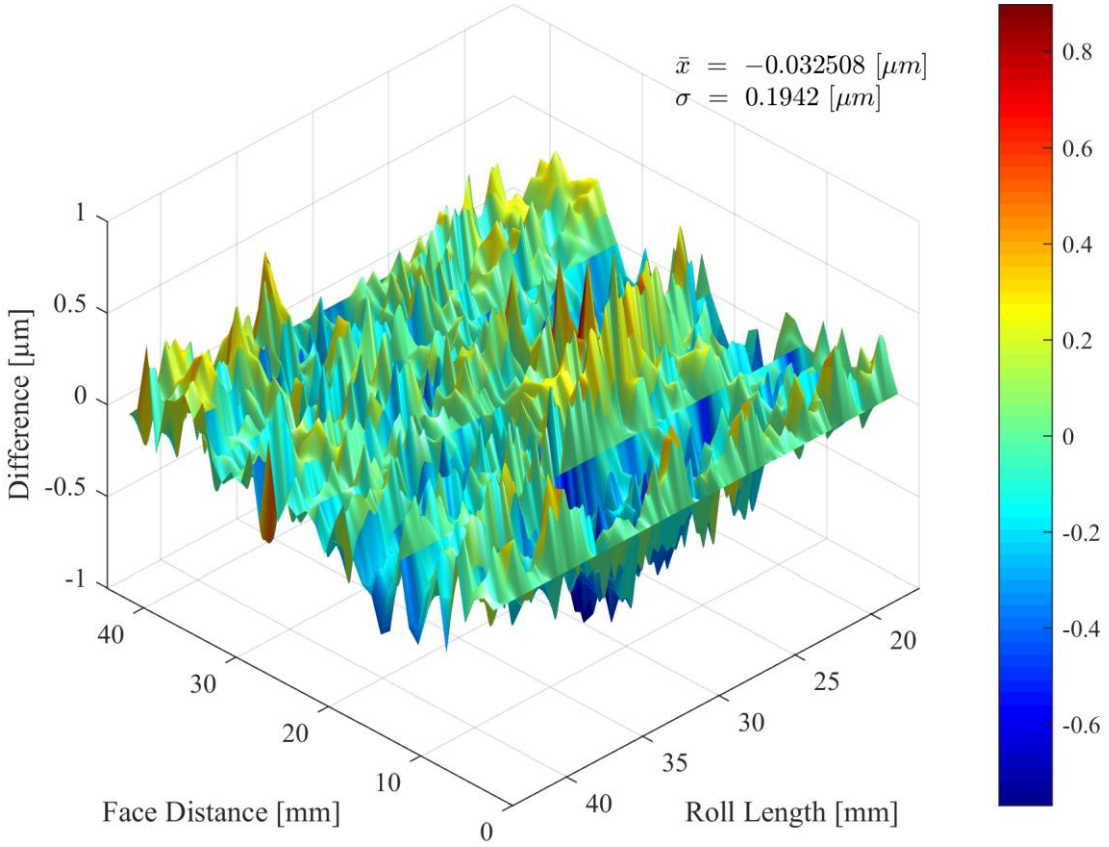

Figure 12: Difference between the topography and linear interpolated surfaces. Standard deviation of the difference σ = 0.19 µm.

Equivalent approach is followed with the Gaussian interpolation of the waviness, see Figure 13. The resulting interpolated surface is illustrated in Figure 14 and the difference between the topography and interpolated surfaces is illustrated in Figure 15.

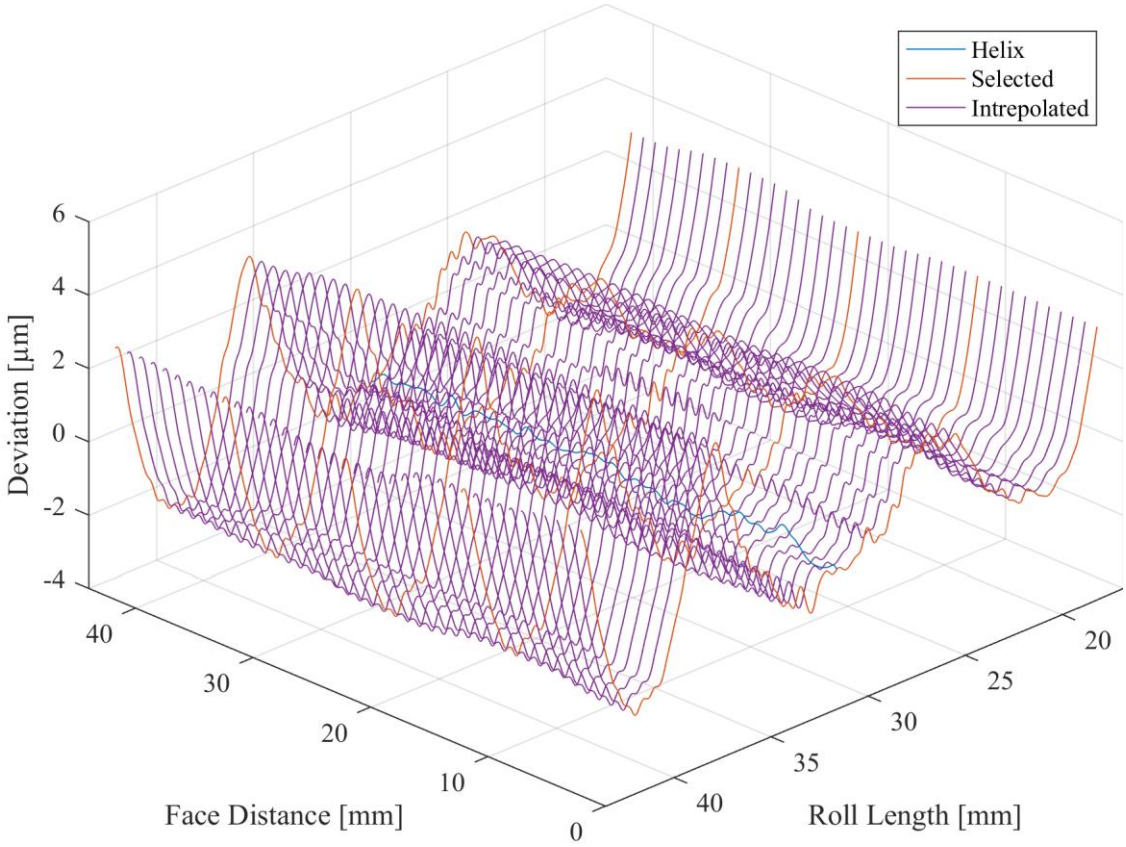

Figure 13: Waviness residual after removing $S_{55}(b, \rho)$ description of the form. Gaussian interpolation of the waviness is also shown.

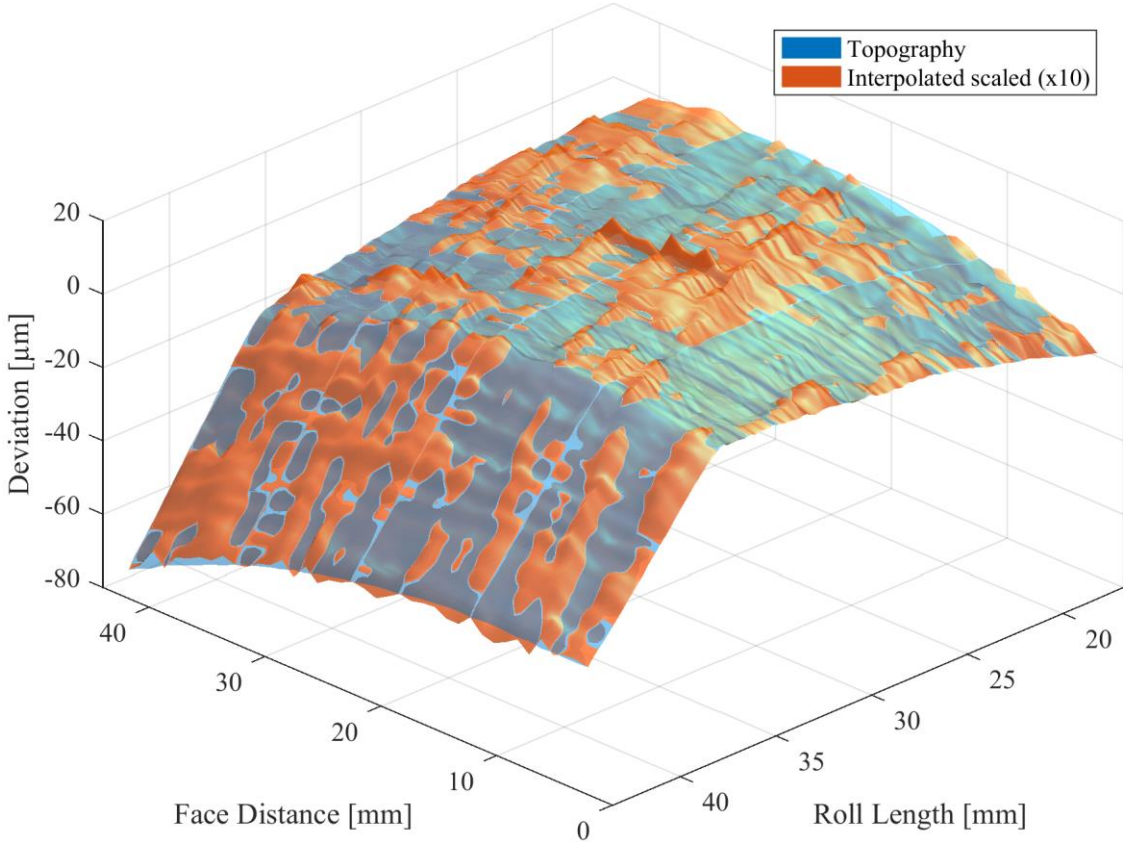

Figure 14: Topography and Gaussian interpolated flank surfaces with form removal. The deviations of the interpolated surface have been scaled by factor of 10 with respect to the topography surface.

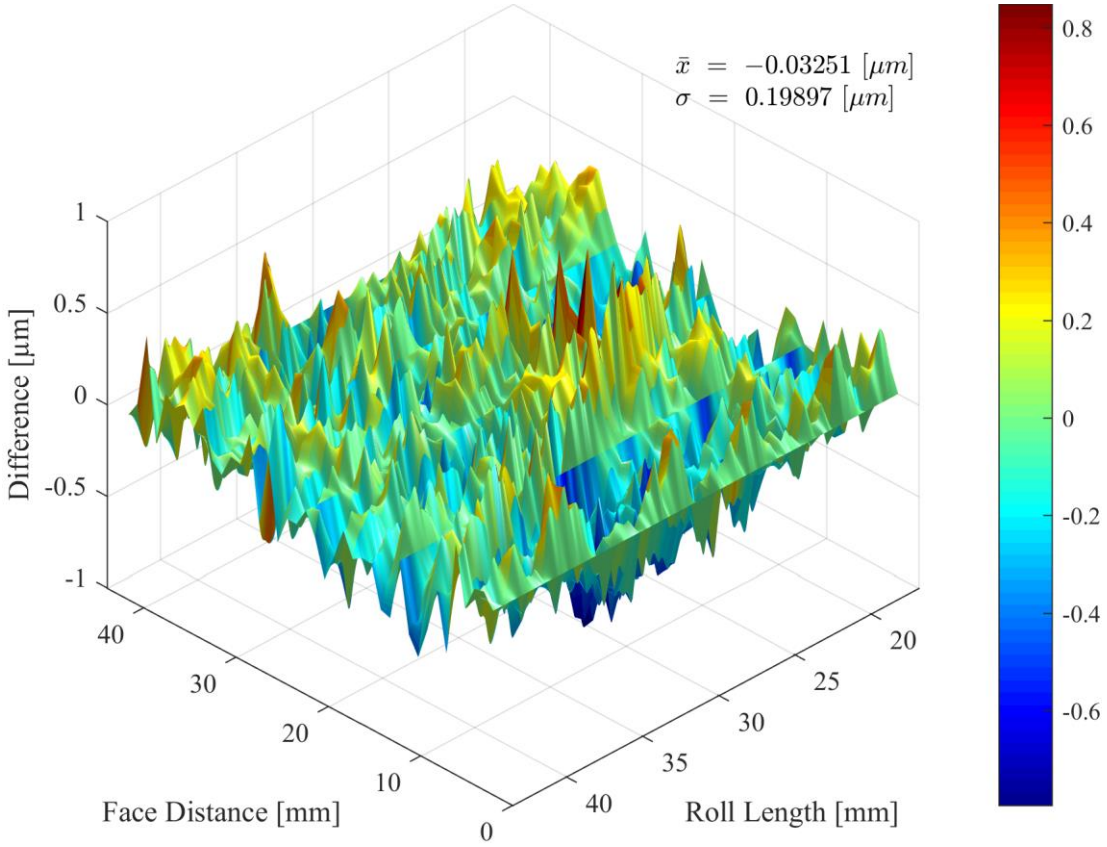

Figure 15: Difference between the topography and Gaussian interpolated surfaces. Standard deviation of the difference σ = 0.20 µm.

Removing the form prior to interpolation has reduced the standard deviation of the difference from 0.31 µm to 0.19 µm and from 1.11 µm to 0.20 µm for linear and Gaussian interpolation, respectively. Form removal works well on this directional ground surface, reducing the discrepancy between linear and Gaussian interpolation.

3.3 Interpolation for varying number for profiles

The aim of this method is to characterise the helical gear flank surface economically with the minimum number of measurements. It is possible to interpolate the surface with reduced number of measured profiles. The interpolated surface which is produced from smallest number of individual measurements yet still satisfies the quality criterion is deemed most economically interpolated.

The quality of the interpolated surface should not have a dominant contribution to the overall measurement uncertainty. The uncertainty contribution resulting from the interpolation can be estimated as the standard deviation of the difference between the interpolated and topography surfaces. The assumption is made that the topography surface sufficiently represents the measured surface. The maximum overall expanded uncertainty $U(k=2)$ of the measurement is ± 1.3 µm, as stated in section 2.1. The uncertainty contributions are typically added in quadrature, meaning taking the square root of the sum of the squared contributions. For a contribution to have minimal effect on the overall value it

must be of similar order as the overall value. Therefore the quality criterion is defined such that the expanded uncertainty contribution from the interpolation method must be less than the overall expanded uncertainty of the measurement, which was chosen to be less than 1 µm in this case. This value is used to define the quality threshold, see Figure 17.

The reasonable limit for the minimum number of profiles is three, which corresponds to the twist check measurement used in the industry. The reasonable limit for the maximum number of profiles is twenty, which is half of the data available from the topography measurement. Polynomial surface equation $S_{33}(b, \rho)$ was used to describe the form of the measured data for this part of the study, illustrated in Figure 16. This surface polynomial was chosen since it provided a stable polynomial fitting solution even with three measured profiles. Higher order surface polynomial fitting result was unstable and erroneous.

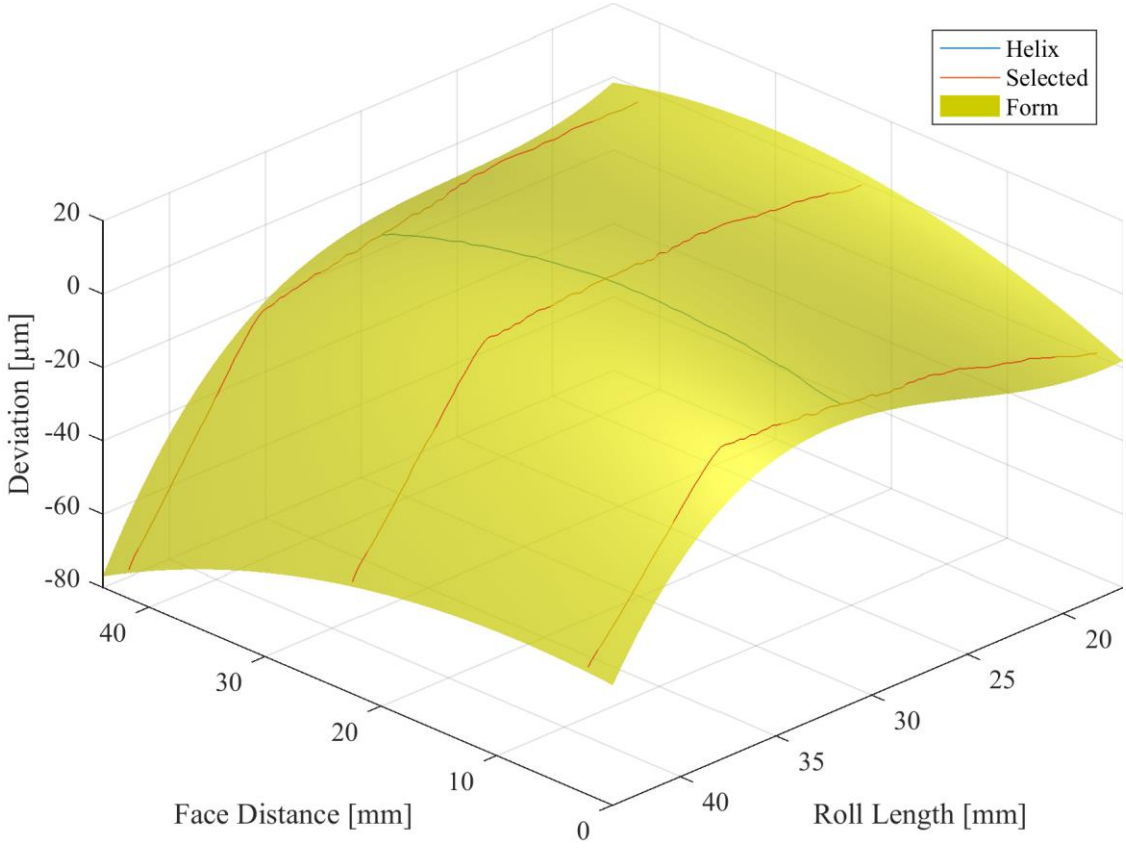

Figure 16: $S_{33}(b, \rho)$ surface polynomial fit of the form with three profile and a single helix measurements.

The presented interpolation methodology was applied to cases of varying numbers of measured profiles for both interpolation with and without form removal. The resulting standard deviation of the difference between interpolated and topography surfaces for varying number of measured profiles is illustrated in Figure 17. The quality threshold of 0.5 µm is displayed which corresponds to expanded uncertainty of ± 1 µm. The interpolation results with the minimum number of measured profiles yet satisfying the quality criterion are summarised in

Table 3.

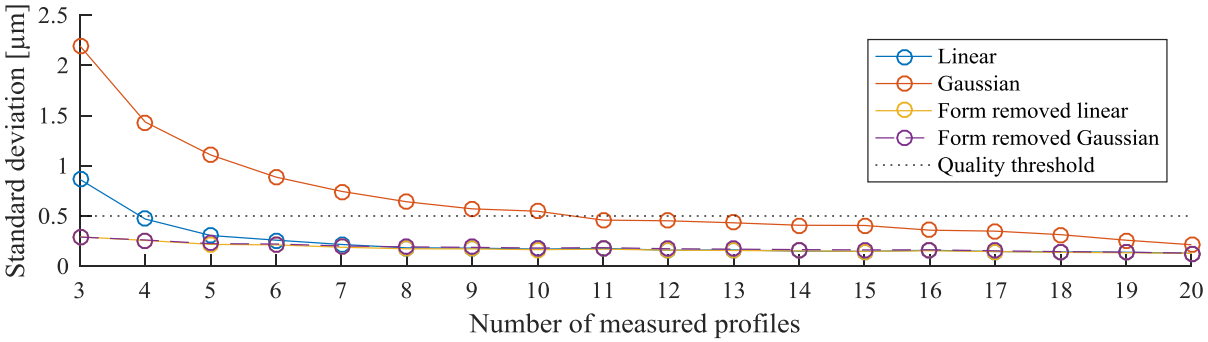

Figure 17: Comparison of the linear and Gaussian interpolation with and without form removal. Comparison is made by the standard deviation of the difference between topography and interpolated surfaces illustrated on the vertical axis. The number of measured profiles used to interpolate the surface is illustrated along the horizontal axis. The quality threshold is at 0.5 µm which corresponds to expanded uncertainty $U(k=2)$ of ± 1 µm.

Table 3: Interpolation results satisfying the quality criterion with minimum number of measured profiles.

Interpolation	Form removal	Number of measured profiles	Standard deviation [µm]	Expanded uncertainty $U(k=2)$ [µm]
Linear	none	4	0.47	0.94
Gaussian		11	0.46	0.92
Linear	$S_{33}(b,\rho)$	3	0.29	0.58
Gaussian		3	0.29	0.58

It can be seen that the application of the interpolation with form removal dramatically improves the quality of the interpolated surface and reduced the number of needed measurements. This is specifically advantageous for large face width gears where minimising the number of required measurements will significantly increase inspection times.

4 Conclusions

A methodology for interpolation of helical gear flank surface from sparse line measurements has been presented. The method has been applied to a precision ground gear with profile and helix modifications and significant manufacturing errors. The approach of quantifying the quality of the interpolated surface in terms of measurement uncertainty contribution has been followed. The definition of quality criterion allows identification of the minimum number of single line measurements needed to sufficiently and economically characterise the surface.

Three profiles and a single helix measurements is sufficient to reconstruct the gear flank surface for the case presented. This is deemed an economical method for gear flank surface characterisation and provides valuable information that could be used to evaluate the manufactured gear performance, for example by means of TCA.

The TCA can be used to develop functionality and performance based characterisation parameters, consistent with the requirements of GPS compatible measurement strategies. The method can also be used by designers to decide whether the level of performance resulting from actual manufacturing errors is acceptable, which in some cases could be used to justify acceptance of components which would normally be rejected based on general specified geometrical tolerances.

Acknowledgements

The authors acknowledge the European Metrology Research Programme (EMRP). The EMRP is jointly funded by the EMRP participating countries within EURAMET and the European Union. This work was done as part of EMRP collaborative project ENG56.

References

[1] *BS ISO 1328-1:2013 Cylindrical gears — ISO system of flank tolerance classification*. 2013, British Standards Institution: London.
[2] *BS EN ISO 6336-1:2006 Calculation of load capacity of spur and helical gears — Part 1: Basic principles, introduction and general influence factors*. 2006, British Standards Institution: London.
[3] *BS ISO 17450-1:2011 Geometrical product specifications (GPS) — General concepts. Part 1: Model for geometrical specification and verification*. 2011, British Standards Institution: London.
[4] Haddad, C.D., *The Elastic Analysis of Load Distribution in Wide-faced Helical Gears*. 1991, Newcastle upon Tyne: University of Newcastle upon Tyne.
[5] Goch, G. and A. Günther, *Areal Gear Flank Description as a Requirement for Optical Gear Metrology*, in *Towards Synthesis of Micro-/Nano-systems*. 2007, Springer London. p. 47-52.
[6] Lotze, W. and F. Haertig, *3D gear measurement by CMM*. Proceedings of the ‘‘Lamdamap’’, Birmingham, 2001: p. 333-343.
[7] Goch, G., *Gear Metrology*. CIRP Annals - Manufacturing Technology, 2003. **52**(2): p. 659-695.